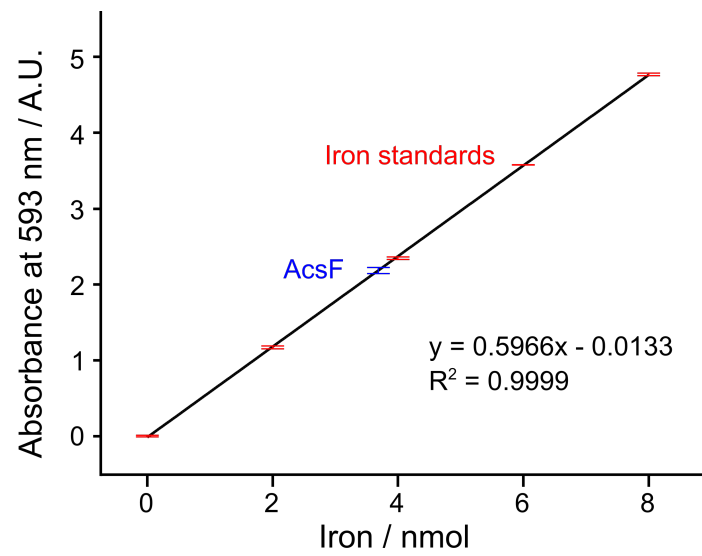
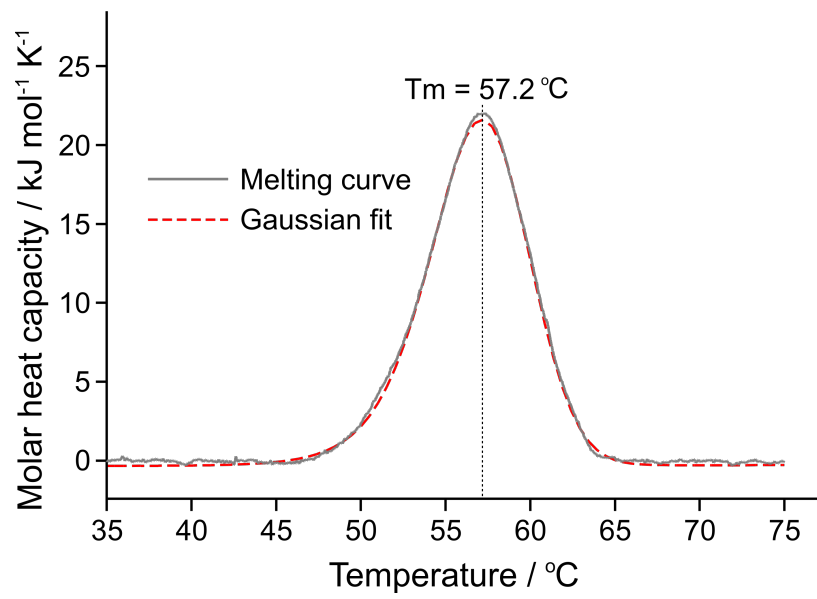


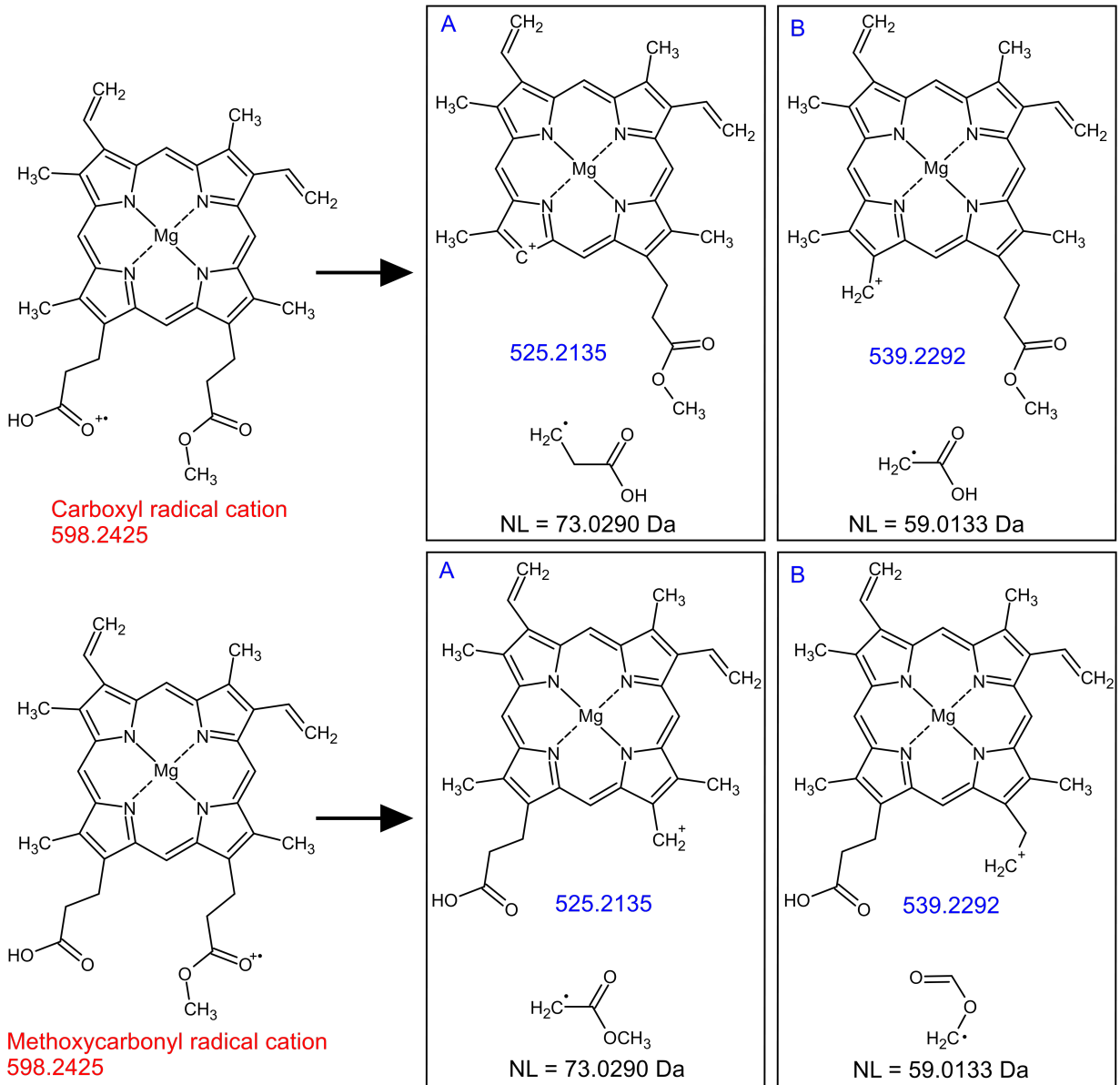
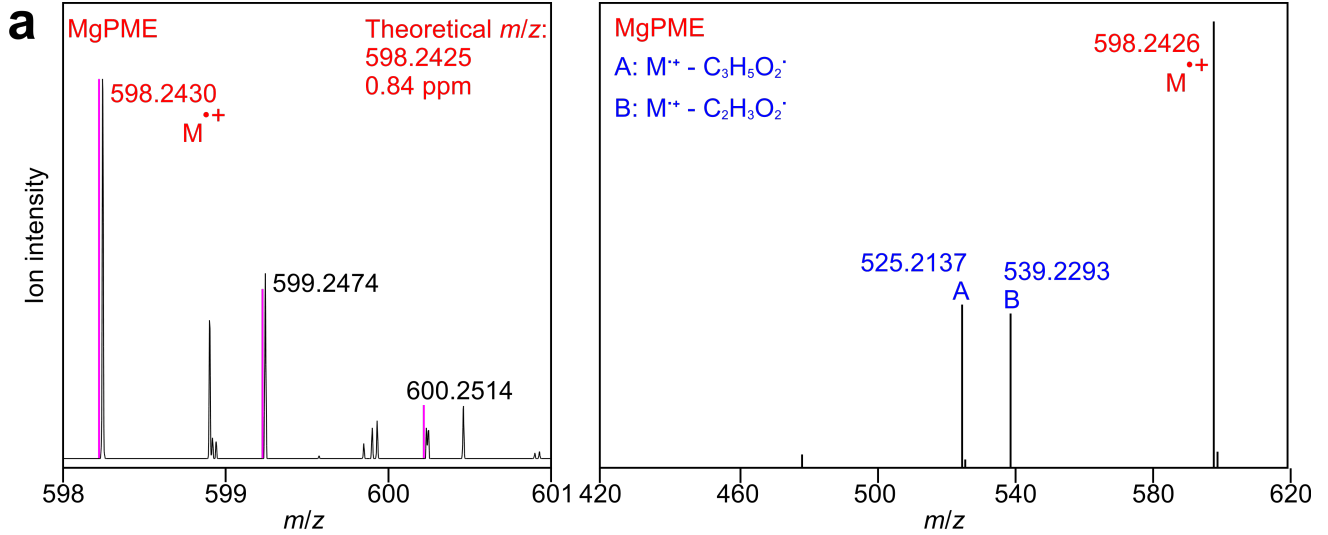
## Supplementary Information

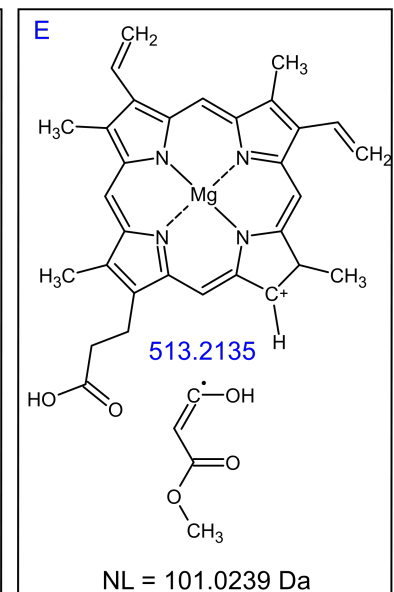
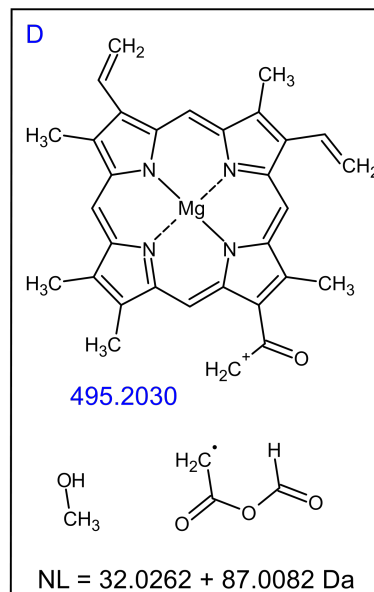
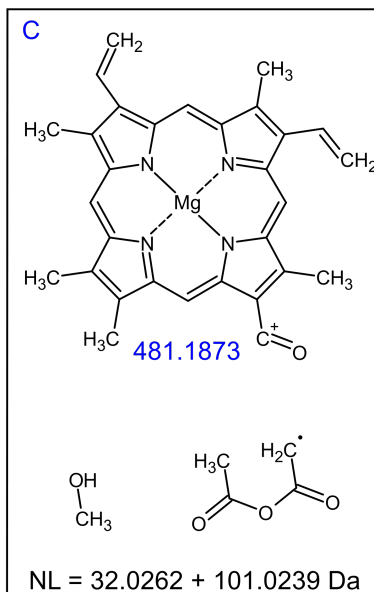
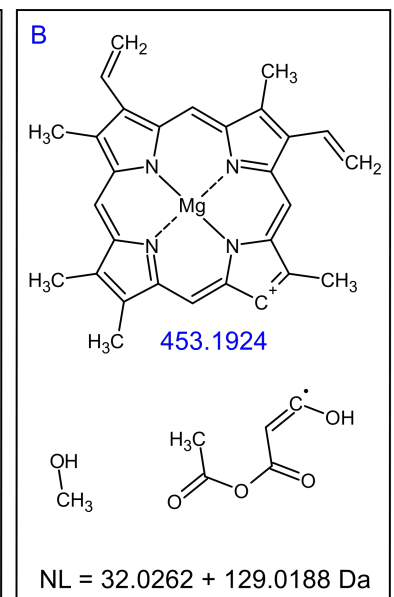
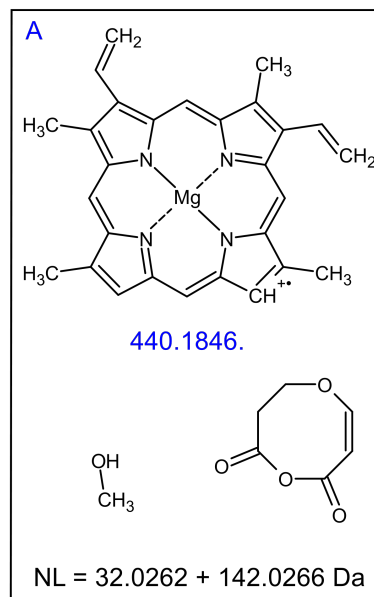
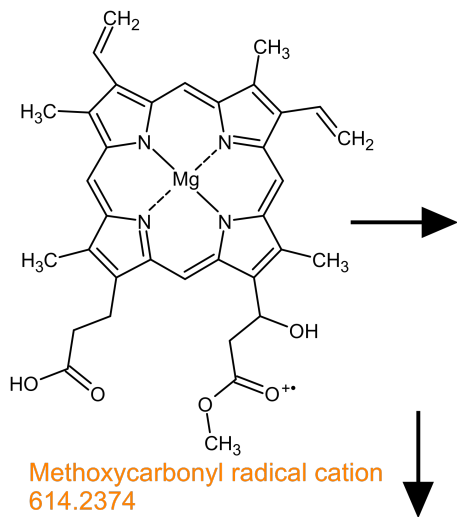
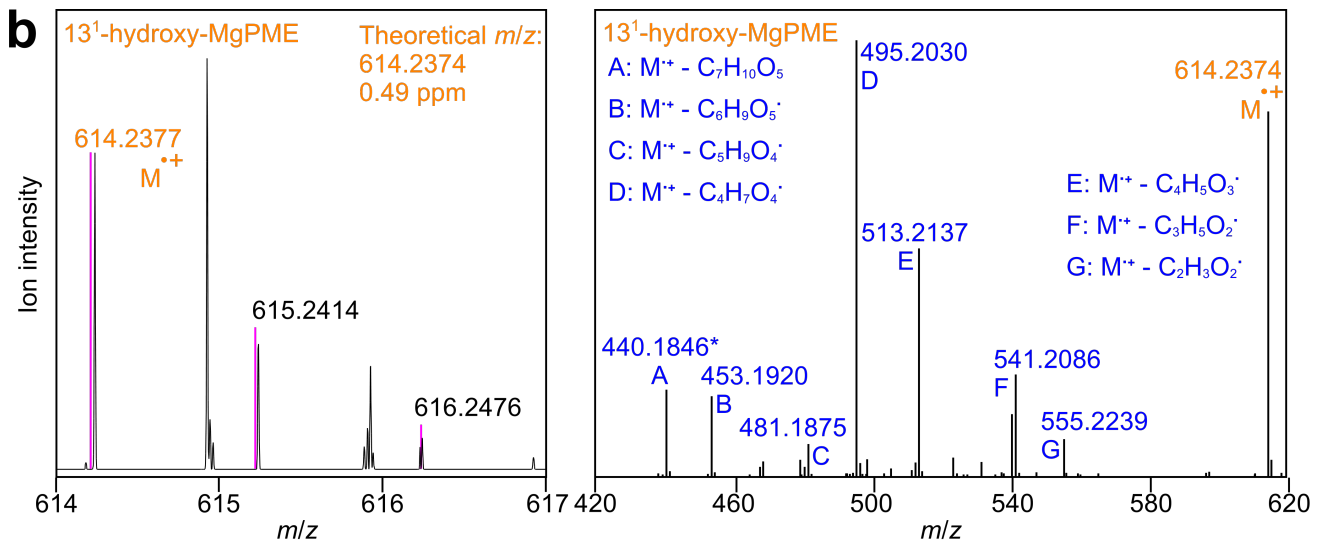


**Supplementary Figure 1. Determination of the iron content of purified AcsF by iron assay.** Error bars indicate the standard deviation from the mean of triplicate experiments. The iron content for 1.569 nmol of AcsF (monomer) was determined to be  $3.684 \pm 0.066$  nmol, producing an iron:AcsF ratio of  $2.35 \pm 0.04$ .

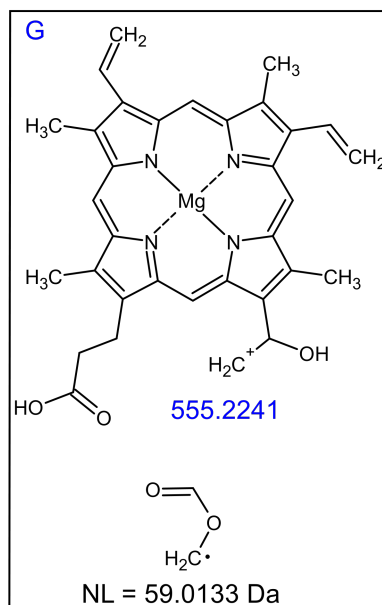
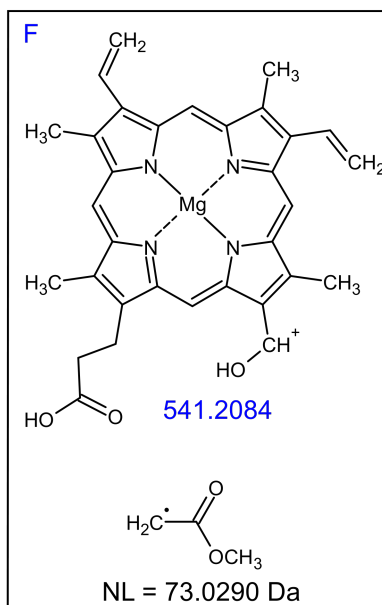
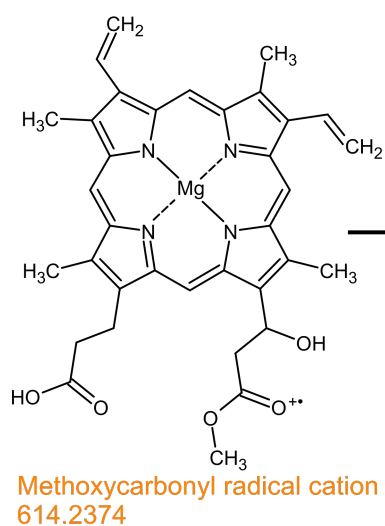
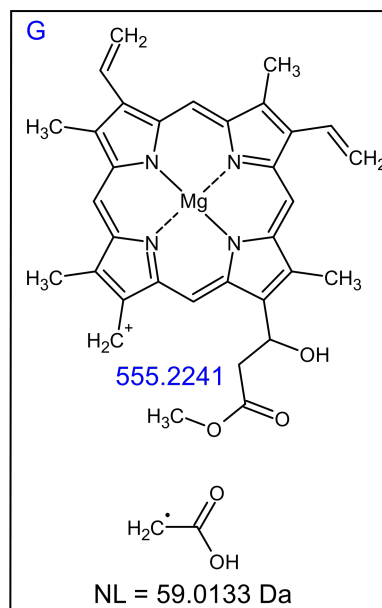
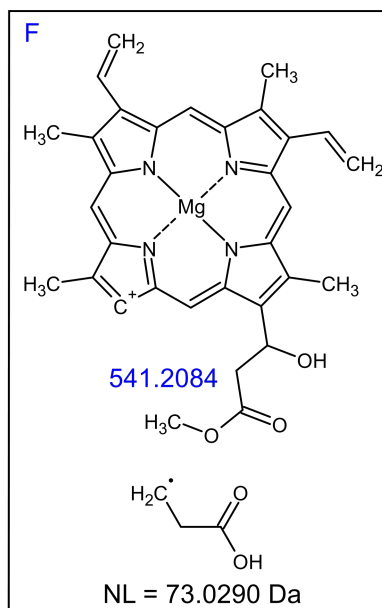
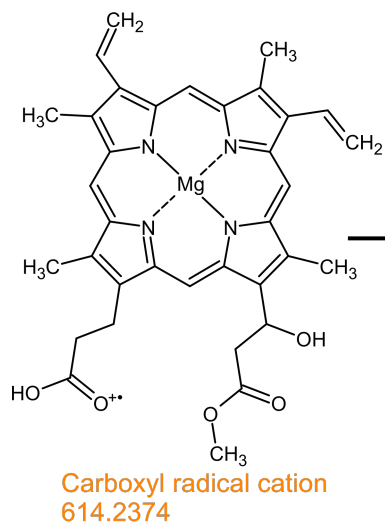


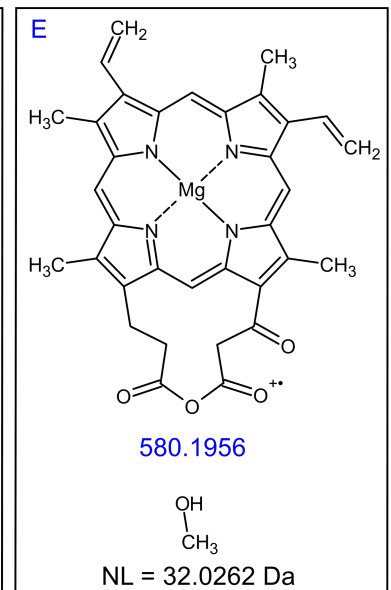
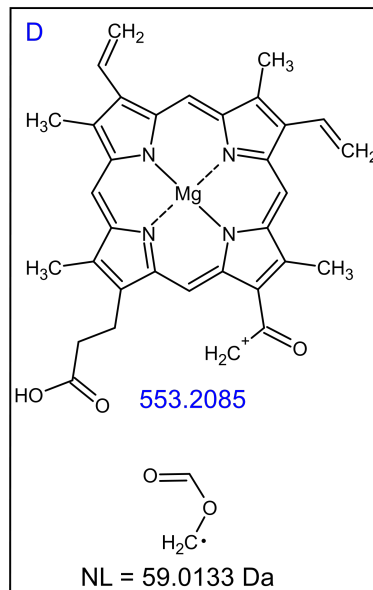
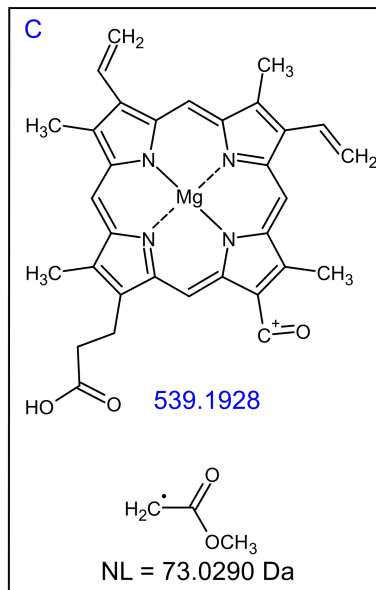
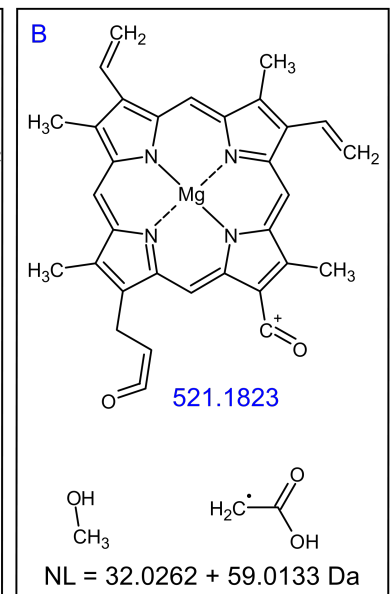
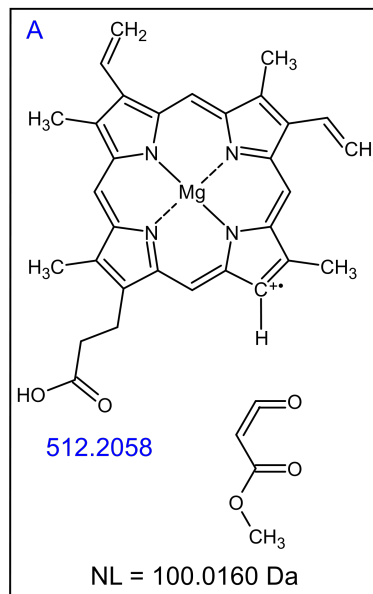
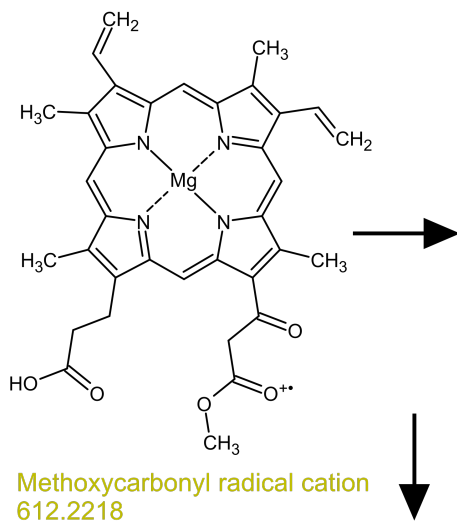
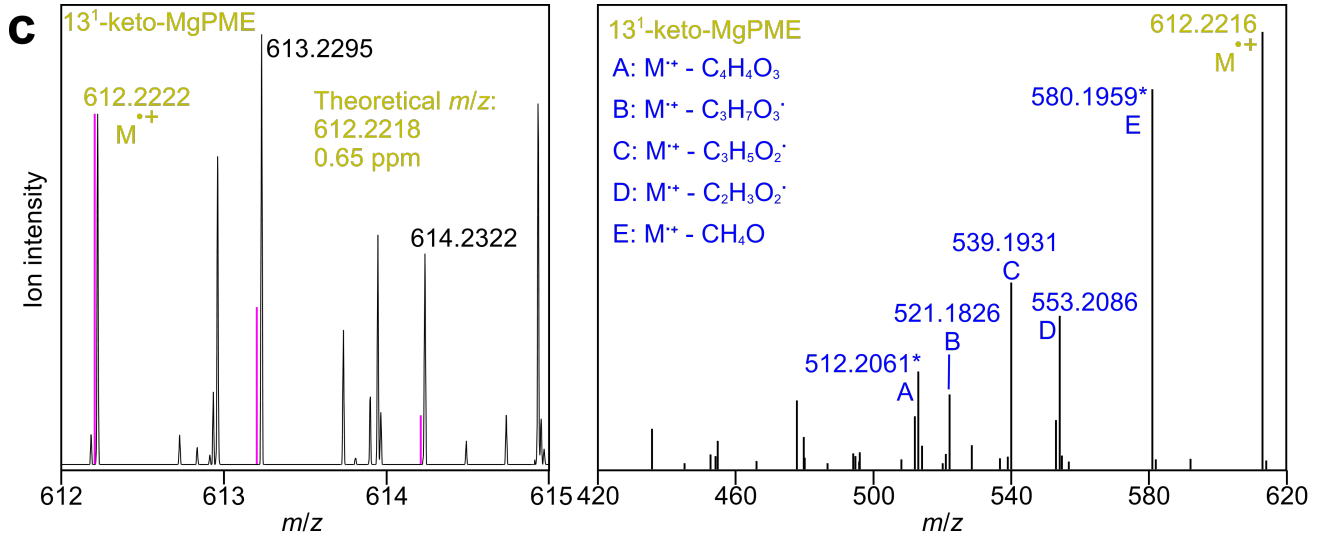
**Supplementary Figure 2. Melting curve of purified AcsF by differential scanning calorimetry analysis.**



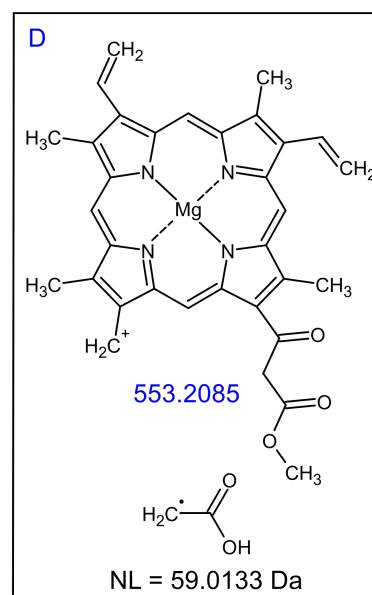
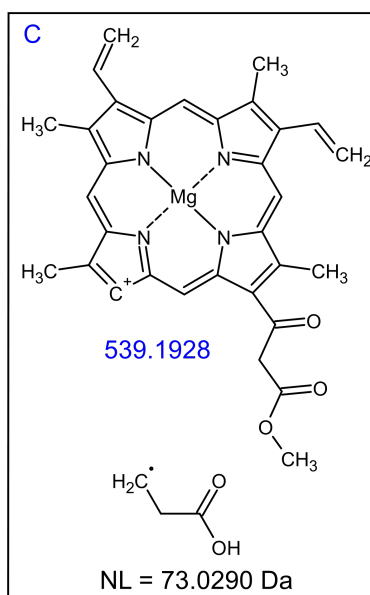
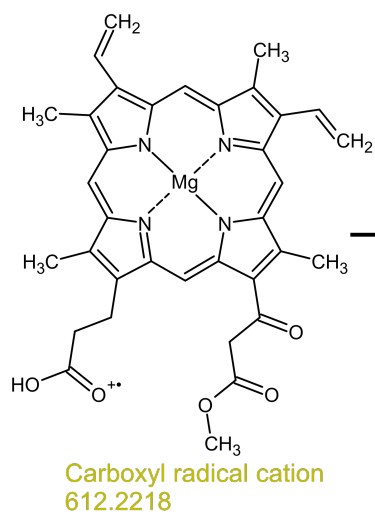


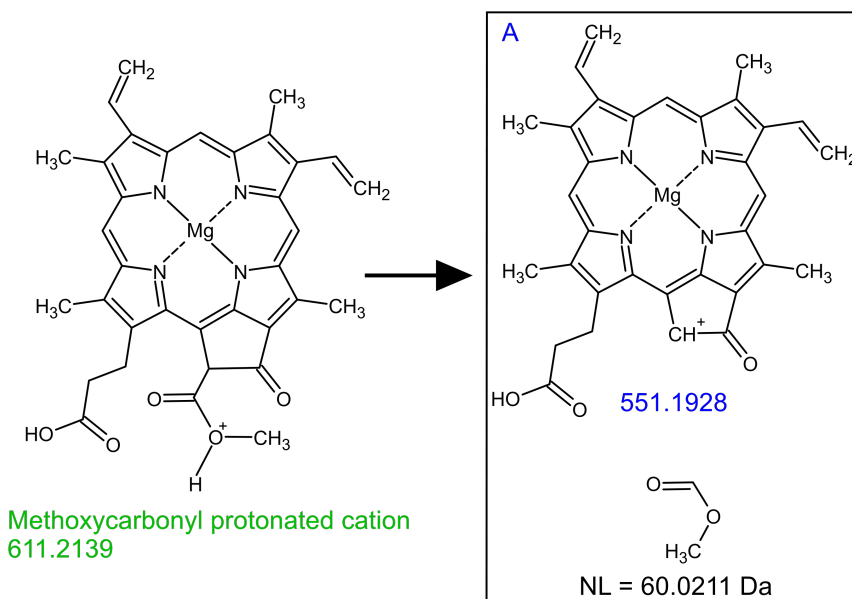
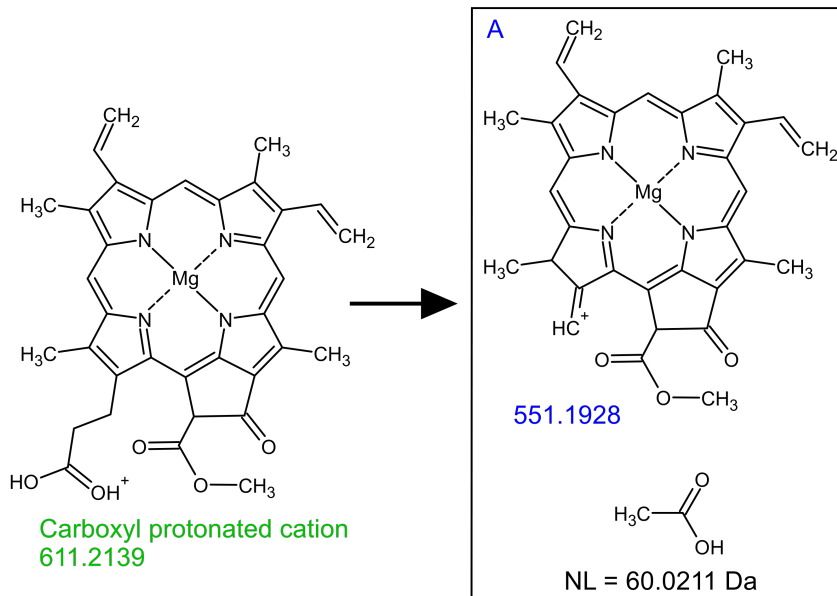
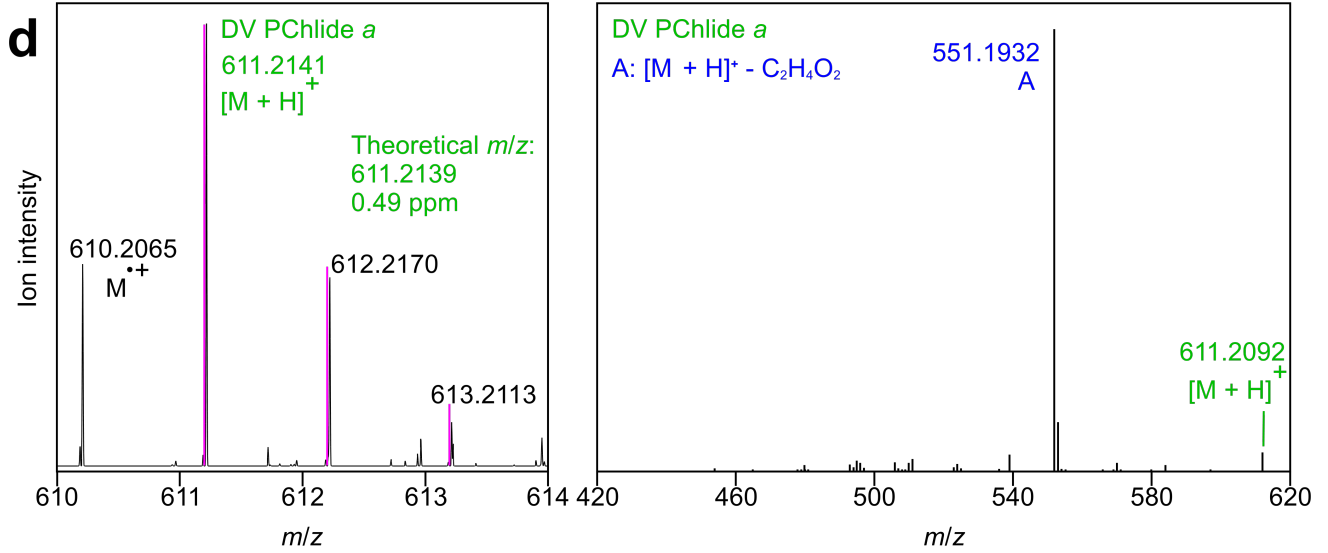
## b (cont.)



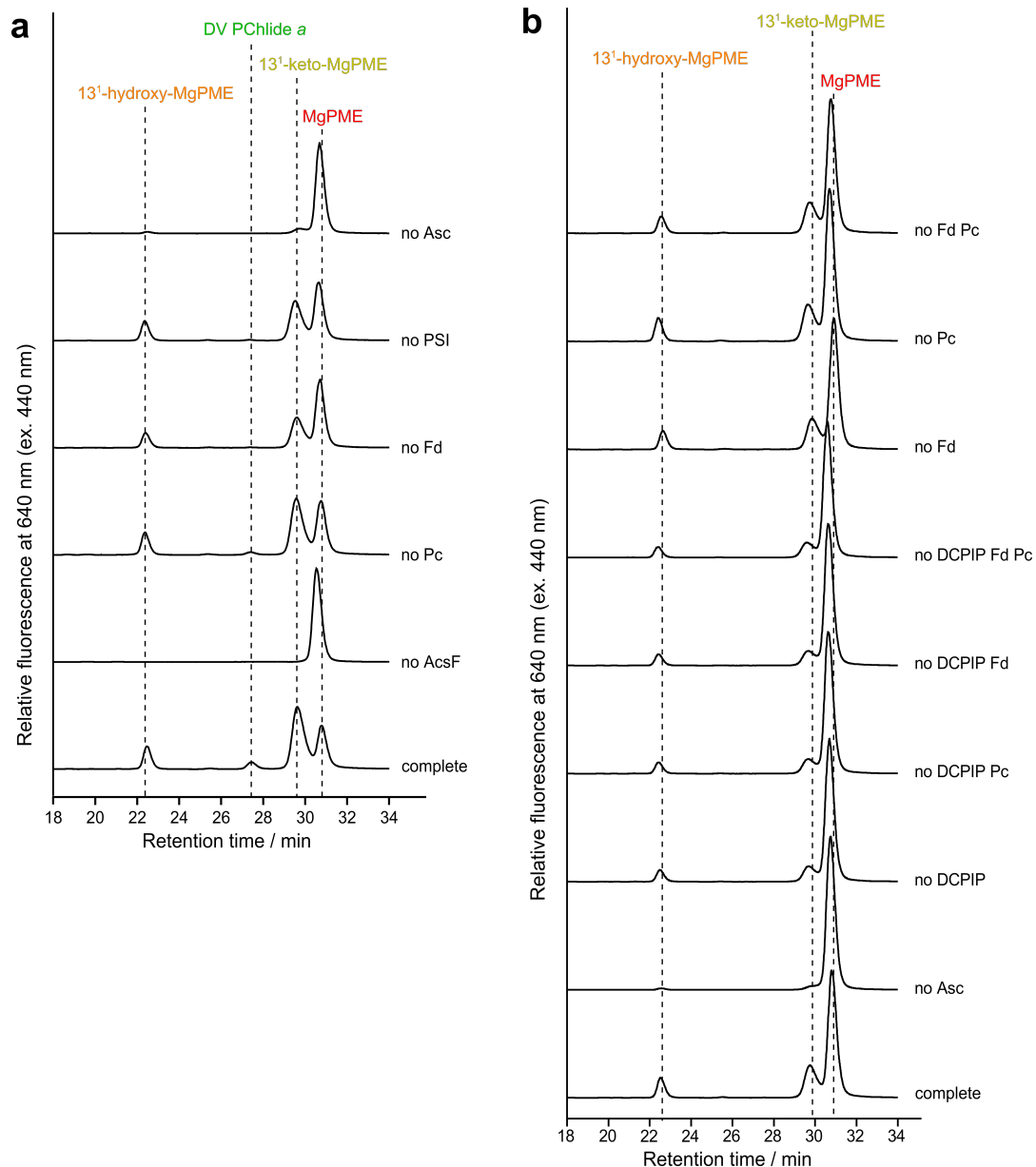


# c (cont.)





**Supplementary Figure 3. Mass spectral evidence for the hydroxy and keto intermediates in the conversion of MgPME into DV PChlide *a*.** Radical cations of MgPME (**a**),  $^{13}\text{C}_1$ -hydroxy-MgPME (**b**) and  $^{13}\text{C}_1$ -keto-MgPME (**c**), and the protonated cation of DV PChlide *a* (**d**) are shown in the full-MS spectra in the *top left* panels labelled with their observed  $m/z$  values and monoisotopic mass accuracies. Also shown in the full-MS spectra are the corresponding  $^{13}\text{C}$  isotopomer ions and theoretical relative isotopomer ion intensities calculated from the molecular formulas (magenta lines). The monoisotopic ions were selected for higher-energy C-trap dissociation in a parallel reaction monitoring experiment to generate the product ion spectra shown in the *top right* panels, also labelled with their observed  $m/z$  values. The *bottom* panels show the proposed molecular structures, represented by single canonical forms and labelled with their theoretical  $m/z$  values, that map to (i) precursor ions identified on the evidence of comparisons between observed and theoretical  $m/z$  values and isotopomer patterns and (ii) dissociation products of the gas phase neutral loss reactions that are evident as  $m/z$  species in the product ion spectra. Our identifications of MgPME and its hydroxy and keto derivatives are consistent with the formation of neutral loss species terminating in either carboxyl or methoxycarbonyl groups, depending on which side-chain carries the unpaired electron, with cleavage of successive C-C bonds up to the tetrapyrrole ring to form, in most cases, carbocations (**aA**, **aB**, **bE–G**, **cC**, **cD**). As expected, there was no evidence of dissociation reactions involving the tetrapyrrole ring itself owing to its stability. To account for some of the dissociation pathways exhibited by  $^{13}\text{C}_1$ -hydroxy-MgPME (**b**) and  $^{13}\text{C}_1$ -keto-MgPME (**c**) it is probable that an even electron neutral loss of methanol forms an anhydride intermediate that subsequently either undergoes further dissociation (**bA–D**, **cB**) or occurs as a radical cation (**cE**). The dissociation pathways for the protonated cation of DV PChlide *a* that would generate acetic acid and methyl formate, both at 60.0211 Da are shown in **d**. It is proposed, however, that the only significant tetrapyrrole product carbocation detected is from the neutral loss of methyl formate from the methoxycarbonyl radical cation. If the unpaired electron had resided on the carboxyl group, we would have expected to see carbocation products at both 551.1928 and 537.1724  $m/z$ , the latter resulting from the neutral loss of propionic acid as seen in the dissociation reactions for MgPME,  $^{13}\text{C}_1$ -hydroxy-MgPME and  $^{13}\text{C}_1$ -keto-MgPME (**aA**, **bF**, **cC**). It is therefore apparent that the formation of the isocyclic ring directs preferential protonation of the attached methoxycarbonyl group and, consistent with its expected stability, does not dissociate under the conditions used in this analysis thus restricting the potential number of neutral losses to one. All  $m/z$  assignments, in terms of odd and even integer masses follow the Nitrogen Rule, i.e. molecules containing an even number of N atoms (like tetrapyrroles) form even electron ions with odd integer masses and vice versa. The majority of tetrapyrrole product ions detected here are even electron carbocations with odd integer masses. The three occurrences of odd electron radical cation products with even integer masses are marked with an asterisk. The spectral peaks at 613.2295 and 614.2322  $m/z$  in **c** are more intense than would be expected for the  $^{13}\text{C}_1$  and  $^{13}\text{C}_2$  isotopomer ions (theoretical intensities are shown by magenta lines) owing to the presence of merged unidentified coincident ions.



**Supplementary Figure 4. HPLC analysis of pigment extracts from coupled PSI-cyclase assay controls.**

Pigment extracts from assays were analysed by HPLC with pigment elution monitored by fluorescence at 640 nm with excitation at 440 nm. Pigment species were identified by retention times and fluorescence spectra (as in Fig. 4). **a**, Cofactor requirements for cyclase activity in the coupled PSI-cyclase assays. A complete assay contained 2  $\mu\text{M}$  AcsF, 0.04  $\text{mg mL}^{-1}$  spinach Fd, 14  $\mu\text{M}$  MgPME, spinach PSI containing 6  $\mu\text{M}$  Chl *a*, 20  $\mu\text{M}$  spinach Pc, 2 mM Asc, 60  $\mu\text{M}$  DCPIP and 0.29  $\text{mg mL}^{-1}$  catalase. Assays were incubated under red light illumination for 30 min. **b**, Partial cyclase activity in the absence of PSI. A complete assay contained 2  $\mu\text{M}$  AcsF, 0.06  $\text{mg mL}^{-1}$  spinach Fd, 14  $\mu\text{M}$  MgPME, 20  $\mu\text{M}$  spinach Pc, 3 mM Asc, 60  $\mu\text{M}$  DCPIP and 0.29  $\text{mg mL}^{-1}$  catalase. Assays were incubated in the dark for 30 min.

**Supplementary Table 1. Nucleotide sequences of synthesised genes used in this study\*.**

Gene	Sequence (5'-3')
<i>petF</i>	ATGGCTACTTTCAAAGTTACCTTGATCAACGAGGCAGAAGGGACTAAGCATGAAATCGAGGTTCCAGAC GACGAGTACATCCTTGATGCGGCAGAGGAACAGGGCTATGATTTGCCCTTTTCATGCCGCGCAGGTGCA TGTTCCACATGCGCCGGTAAGTTGGTATCGGGCACTGTAGACCAATCGGATCAAAGTTTCTGGACGAC GACCAAATTGAAGCCGGCTACGTCCTGACTTGTGTGCGTTATCCGACATCAGATGTAGTTATCCAAACG CACAAAGAGGAAGATTTGTATTAA
<i>petH</i>	ATGGGTACCCAGGCTAAAGCCAAGCACGCTGACGTTCCCTGTCAATCTTTACCGCCCAAATGCCCCCTTC ATCGGCAAGGTGATCTCAAACGAACCCTTAGTGAAGGAGGGAGGCATTGGAATTGTTTCAGCACATTTAAA TTTGATCTTACAGGCGGAAACTTAAAGTACATCGAGGGGCAGTCAATCGGCATTATTCGCCCCGGCGTA GACAAAAATGGCAAGCCTGAAAAATTACGTTTGTATTCTATTGCAAGCACTCGTCACGGTGATGATGTG GATGATAAAACTATTTCCCTGTGCGTCCGCCAACTGGAGTATAAGCATCCCGAGTCAGGAGAAACGGTG TACGGAGTCTGCTCTACGTACCTTACTCACATTGAGCCGGGATCTGAAGTTAAAAATTACCGCCCTGTG GGGAAGGAAATGCTGTTGCCAGATGATCCAGAGGCTAACGTTATCATGTTGGCAACCGGGACCGGTATC GCCCCATGCGTACCTACTTGTGGCGTATGTTTAAGGACGCAGAACGTGCCGCTAACCCGGAGTATCAA TTCAAGGGGTTTCAGTTGGCTTGTTCGGAGTCCCAACGACTCCGAATATCTTATAACAAGGAAGAGTTG GAGGAGATCCAACAAAAGTACCCTGATAACTTTCGTCTTACCTACGCTATCTCCCGTGAGCAGAAAAAT CCCCAGGGCGGTTCGTATGTATATTCAGGACCGCGTGGCAGAACACGCGGACGAGTTATGGCAGCTGATT AAAAATCAAAGACACACACGTATATTTGTGGCCTTCGCGGAATGGAAGAGGGAATTGACGCTGCTCTG TCGGCTGCTGCTGCCAAGGAGGGTGTACTTGGTTCGGACTACCAGAAGGATCTTAAGAAGGCCGGACGC TGGCATGTAGAGACTTACTAA

\*Genes are codon optimised for expression in *E. coli*. The *petF* gene encodes the *Anabaena* Fd. The *petH* gene encodes the *Anabaena* FNR lacking the N-terminal 136 aa. For cloning reason, a GGT sequence (underlined) was added to the *petH* gene, which encodes a Gly at aa position #2.